The Astronomical Journal, 155:246 (10pp), 2018 June https://doi.org/10.3847/1538-3881/aac01f

Bi-lobed Shape of Comet 67P from a Collapsed Binary

David Nesvorný[1], Joel Parker[1], and David Vokrouhlický[1,2]
[1] Department of Space Studies, Southwest Research Institute, 1050 Walnut Street, Suite 300, Boulder, CO, 80302, USA
[2] Institute of Astronomy, Charles University, V Holešovičkách 2, CZ-18000 Prague 8, Czech Republic
Received 2018 February 5; revised 2018 April 20; accepted 2018 April 23; published 2018 May 22

Abstract

The Rosetta spacecraft observations revealed that the nucleus of comet 67P/Churyumov–Gerasimenko consists of two similarly sized lobes connected by a narrow neck. Here, we evaluate the possibility that 67P is a collapsed binary. We assume that the progenitor of 67P was a binary and consider various physical mechanisms that could have brought the binary components together, including small-scale impacts and gravitational encounters with planets. We find that 67P could be a primordial body (i.e., not a collisional fragment) if the outer planetesimal disk lasted $\lesssim$10 Myr before it was dispersed by migrating Neptune. The probability of binary collapse by impact is $\simeq$30% for tightly bound binaries. Most km-class binaries become collisionally dissolved. Roughly 10% of the surviving binaries later evolve to become contact binaries during the disk dispersal, when bodies suffer gravitational encounters with Neptune. Overall, the processes described in this work do not seem to be efficient enough to explain the large fraction ($\sim$67%) of bi-lobed cometary nuclei inferred from spacecraft imaging.

Key words: comets: individual (67P/Churyumov–Gerasimenko)

1. Introduction

The spectacular images of Rosetta's OSIRIS camera revealed that the nucleus of comet 67P/Churyumov–Gerasimenko has a bi-lobed shape (Figure 1). The dimensions of the small and large lobes are $2.5 \times 2.1 \times 1.6$ km and $4.1 \times 3.5 \times 1.6$ km, respectively (Jorda et al. 2016). Their volume ratio is 2.4. The two lobes are connected by a narrow neck giving 67P appearance of a contact binary. Several recent studies addressed the question of the origin of the 67P shape. Jutzi & Benz (2017) suggested that 67P formed as a result of the low-energy, sub-catastrophic impact on an elongated, rotating parent body. Schwartz et al. (2018) proposed, instead, that 67P and other bilobate comets formed during catastrophic collisional disruptions of much lager bodies. Another possibility, which we investigate in this work, is that 67P formed as a binary planetesimal that subsequently collapsed to become a contact binary (Rickman et al. 2015).

Opinions differ about whether 67P is primordial (i.e., formed as a small cometesimal by some accretion process 4.6 Gyr ago) or whether it was once part of a larger parent planetesimal and was liberated from it by an energetic impact. Morbidelli & Rickman (2015, hereafter MR15) studied the collisional survival of 67P in a massive outer disk at 15–30 au, which is thought to be the ultimate source of comets (Nesvorný et al. 2017). They found that an object of the size of 67P should suffer tens of catastrophic collisions over the assumed disk lifetime (400 Myr). The survival probability would be negligible in this case ($<10^{-4}$). The disk lifetime, however, may have been shorter (Jutzi et al. 2017 and discussion in Section 2). The survival of 67P after the outer disk dispersal, during the stage when 67P spent >4 Gyr in the scattered disk, is less of an issue.

Davidsson et al. (2016), on the other hand, argued that 67P is a primordial rubble pile that somehow, perhaps because the outer disk remained dynamically cold, avoided being shattered by impacts. They pointed out that the surfaces of both lobes are characterized by thick layers that envelope the lobes individually (Massironi et al. 2015). If the layering was produced during the accretion of 67P, then its existence indicates that 67P somehow avoided being collisionally disrupted, in contradiction to the conclusions of MR15. This would suggest, among other things, that the final stage of the 67P nucleus formation was a gentle merger between two similarly sized cometesimals (Rickman et al. 2015).

Blum et al. (2017) took the arguments of Davidsson et al. a step further, proposing that 67P formed via a gravitational collapse of a bound clump of pebbles. The gravitational collapse, which can be triggered by the streaming instability in a protoplanetary disk (Youdin & Goodman 2005), is a model for the formation of planetesimals that gained substantial support in the recent years (e.g., Youdin & Johansen 2007; Johansen et al. 2009, 2012; Nesvorný et al. 2010; Simon et al. 2017). Blum et al. (2017) pointed out that this formation model is compatible with several properties of 67P, including the global porosity, homogeneity, tensile strength, thermal inertia, and sizes and porosities of the emitted dust particles.

Here, we evaluate the possibility that the bi-lobed shape of 67P emerged in two steps: (1) 67P's parent binary formed by the gravitational collapse of pebbles (Nesvorný et al. 2010) or by some other mechanism (e.g., Goldreich et al. 2002), and (2) the parent binary was destabilized leading to a gentle collision between the binary components.

As for (1), the binaries with similarly sized components are common in the dynamically cold population of the classical Kuiper Belt at 40–50 au (the so-called Cold Classicals or CCs; Noll et al. 2008). Here, we assume that analogous binaries formed in the massive planetesimal disk at 15–30 au. This is reasonable because the planetesimal accretion in the outer solar system should have been controlled by the same processes (see, e.g., Youdin & Kenyon 2013 for a review).[3] The volume ratio of 67P's lobes indicates $R_2/R_1 \simeq 0.75$, where R_1 and R_2 are the effective radii of the two lobes. This turns out to be a common value among the known CC binaries and is also found to be

[3] Note that loosely bound binaries do not survive gravitational encounters with Neptune during the dynamical implantation of bodies into the Kuiper Belt (Parker & Kavelaars 2010). That is why only a very few wide, equal-size binaries were detected in the dynamically hot population of the Kuiper Belt.

Figure 1. Comet 67P/Churyumov–Gerasimenko as imaged by the OSIRIS camera onboard of the Rosetta spacecraft on 2014 August 3. Credit: ESA/Rosetta/MPS and the OSIRIS team.

right in the middle of the values expected from the gravitational collapse (Nesvorný et al. 2010).

As for (2), the parent binary of 67P could have been destabilized by small impacts that transferred the linear momentum of the projectile to binary components. Alternatively, it could have been destabilized dynamically by gravitational encounters with planets (during the implantation of cometesimals into cometary reservoirs or later transfer of bodies from the cometary reservoirs into the inner solar system), or by the Kozai cycles (for a binary orbit that had a significant tilt relative to the heliocentric orbit). While many destabilized binaries become unbound, some may end up, after low-speed collisions between components, as contact binaries.

Another possibility is that the bi-lobed shape of 67P formed during the gravitational collapse itself. During the collapse, the pebble cloud fragments and forms bodies of different sizes (Nesvorný et al. 2010). They remain gravitationally bound and collide between themselves at the characteristic speeds of $\simeq$1–10 m s^{-1}, often resulting in accretion. It is therefore possible that the bi-lobed shape of 67P formed as result of such an early merger of two km sized cometesimals that formed within the collapsing cloud. It is not clear, however, whether this process would lead to the formation of contact binaries, or whether the accreted agglomerates would collapse into a more spherical object.

The main difference between this alternative and the two-step process discussed above is the time interval elapsed between: (i) the formation of components, and (ii) their presumed assembly into a contact binary. In the two-step model, there is a significant delay between processes (i) and (ii), possibly as long as $\gtrsim$10 Myr, during which the two components of a binary can gain the internal strength (e.g., by modest radioactive heating) and resist disintegration during their later assembly into a contact binary.

2. Collisional and Dynamical History of 67P

67P is a Jupiter-family comet (JFC) with the semimajor axis $a = 3.46$ au, perihelion distance $q = 1.24$ au, eccentricity $e = 0.64$, inclination $i = 7\overset{\circ}{.}0$, and orbital period $P = 6.4$ years. Its present orbit is unremarkable among JFCs. Several attempts have been made to reconstruct the past dynamical history of 67P. For example, Maquet (2015) numerically integrated the orbit of 67P backward in time. Their integration included the gravitational perturbation of planets, nongravitational forces resulting from 67P's activity, and relativistic effects. They found that 67P suffered a close encounter with Jupiter on 1959 February 4, during which the perihelion distance dropped from $\simeq$2.7 au before the encounter to 1.3 au after the encounter. Another encounter of 67P to Jupiter occurred on 1923 October 2.

Reconstructing the orbital history of 67P much further is difficult because of orbital chaos. At some point, after several Lyapunov times[4] elapse (typically centuries for JFCs), the backward integration behaves much like a forward integration, with the overwhelming majority of orbital clones being ejected from the solar system by Jupiter (Guzzo & Lega 2017). This does not mean, however, that 67P was injected directly onto Jupiter-crossing orbit from some distant reservoir. Instead, the long-term integration tells us only about the *future* evolution of 67P (assuming that it physically survives that long). Therefore, to establish the past dynamical history of 67P, a different approach is needed.

Here, we use the JFC model developed in Nesvorný et al. (2017, hereafter N17). N17 performed full-scale simulations, in which cometary reservoirs were populated in the early solar system and evolved over 4.5 Gyr (see Section 3 for more details). The population of present-day comets obtained in the model was compared with the number and orbits of the known

[4] The Lyapunov time expresses the characteristic timescale for the exponential divergence of nearby orbits. The motion is generally unpredictable on a timescale of several Lyapunov times.

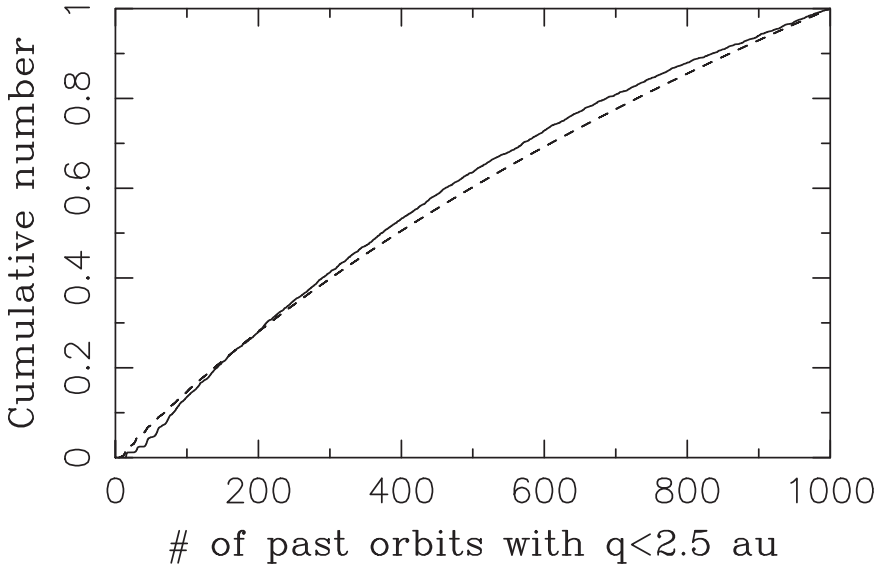

Figure 2. The cumulative distribution of the number of past perihelion passages below 2.5 au. The result for 67P is shown by the solid line. The dashed line shows the distribution for the whole JFC population. Here, we assumed that $N_P(2.5) = 1000$.

JFCs, demonstrating good fidelity of the model. The physical lifetime of model JFCs was parameterized in N17 by the number of perihelion passages below 2.5 au, $N_P(2.5)$, and was constrained from the comparison with the known population of active JFCs (see also Levison & Duncan 1997). The best fit was found to be dependent on the nucleus size. For 67P (effective radius $R \simeq 1.6$ km), this work suggests $N_P(2.5) \sim 1000$, indicating the physical lifetime on an orbit with $q < 2.5$ au of ~5000–10000 years. This is roughly consistent with the measured mass loss of 67P, $\sim 1.8 \times 10^{10}$ kg per orbit (Paetzold et al. 2016). Assuming that this represents the average activity of 67P and that the mass loss is driven by surface processes, the current erosion rate of ~1 meter per orbit indicates that 67P should last ~10000 years.

We selected model JFCs from N17 that reached orbits similar to that of 67P during their dynamical evolution. In practice, the following selection criteria were used: $3.3 < a < 3.6$ au, $0.5 < e < 0.8$ and $5 < i < 9°$. For each model comet, we followed its evolution from the source reservoir (mainly the scattered disk at $50 < a < 150$ au) to the time when the selection was made. We monitored the number of perihelion passages below 2.5 au and the time spent on a JFC orbit after first reaching $q < 2.5$ au. If the number of perihelion passages for an individual comet exceeded 1000 (i.e., $N_P(2.5) = 1000$ using the N17 definition of the physical lifetime), the comet was not considered (assuming that it would cease to be active, either become dormant or disrupt, before it reached the selection time). All other cases were considered together to give us a statistical information about the past evolution history of 67P.

Figure 2 shows the cumulative distribution of the number of past perihelion passages with $q < 2.5$ au of the whole sample. The distribution is broad and has a median of ≃400 perihelion passages with $q < 2.5$ au, corresponding to the median lifetime after first reaching $q < 2.5$ au of $\simeq 10^4$ years (only about one-third of this time is spent on an orbit with $q < 2.5$ au).[5] This shows that 67P probably had hundreds of perihelion passages with $q < 2.5$ au in the past. Therefore, in all likelihood, 67P is *not* a new comet that evolved on a JFC orbit in the past century. The probability that it evolved onto a JFC orbit with $q < 2.5$ au for the first time in the past millennium is only ≃10%.

Using the current mass loss of 67P, ~1 meter per orbit (Paetzold et al. 2016), the above estimates imply that 67P lost, as an order of magnitude estimate, ~400 m of surface layer due to its past activity. If so, the total *initial* volume of 67P, before 67P has become active for the first time, was roughly equivalent to that of a 2 km radius sphere.

As for the collisional survival of 67P, we use the results of MR15 as a guideline. Assuming that 67P formed in the outer planetesimal disk below 30 au (N17) and that the disk lifetime was 400 Myr (i.e., the *late* disk removal), MR15 found that a body of 67P size is expected to suffer 12–40 disruptive collisions. This estimate applies for the cumulative size distribution of projectiles $N(>D) \propto D^q$ with $q = -2$. Steeper (shallower) size distributions lead to a larger (smaller) number of catastrophic collisions.

Recent work suggests that Neptune's migration into the outer planetesimal disk and the disk dispersal happened early, not late (Kaib & Sheppard 2016; Nesvorný et al. 2017b; Morbidelli et al. 2018). If so, the lifetime of the outer disk was shorter than 400 Myr adopted in MR15, possibly much shorter. Assuming, for example, that the disk lifetime was 10 Myr, the number of catastrophic collisions obtained in MR15 would need be divided by a factor of 40. In addition, things depend on the dynamical state of the outer disk, which controls the collisional probabilities and impact speeds. The planetesimal disk is expected to start dynamically cold (in the accretion regime) and be gradually excited by migrating Neptune and ~1000–4000 Pluto-class objects that formed in the disk (Nesvorný & Vokrouhlický 2016). For their nominal estimates, MR15 used the dynamical state of the disk at $t = 300$ Myr from Levison et al. (2011), which may be a good proxy for the long-term average if the planet migration/instability happened at 400 Myr.

If, instead, the planetary migration/instability happened early, the disk remained dynamically cold during much of its

[5] If, instead, we use $N_P(2.5) = 500$, which was the preferred value in N17 for the whole JFC population, the median number of past perihelion passages with $q < 2.5$ au is found to be ≃200.

lifetime. This may contribute by another reduction factor of at least 2 in the number of catastrophic collisions. Also, MR15 assumed, after Brasser & Morbidelli (2013), that there were 2×10^{11} $D > 2.3$ km bodies in the original disk, while the most recent estimates suggest $\simeq 10^{11}$ $D > 2.3$ km cometesimals (N17). Finally, the paucity of small Charon craters (Singer et al. 2018) indicates that the Kuiper Belt may be deficient, relative to $N(>D) \propto D^{-2}$, in small projectiles (diameters $D \lesssim 1$ km). This is significant, because 67P can be collisionally disrupted by sub km projectiles (MR15), and the paucity of these projectiles would imply fewer catastrophic collisions.

The various factors discussed above may reduce the number of catastrophic impacts by at least $\sim 40 \times 2 \times 2 = 160$. On the other hand, in MR15, the specific energy for disruption was taken from the strong ice case and impact speed 1 km s^{-1} in Benz & Asphaug (1999), while 67P is weaker and the impact speeds were lower. It is not clear what a more realistic disruption law should be and how the MR15 results would be modified if that law is used. Jutzi et al. (2017) suggested a disruption law, where a porous target such as 67P is stronger, by at least a factor of ~ 2, than the disruption law from Benz & Asphaug (1999). If so, this would further reduce the number of catastrophic impacts. In any case, taking ~ 100 as a tentative reduction factor, and scaling down from the results of MR15, we find that 67P would experience only 0.1–0.4 disruptive collisions over 10 Myr. If so, the probability to avoid one such collisions is $\exp(-0.1)$ to $\exp(-0.4)$, or 0.7–0.9. Thus, in this case, the survival chances of 67P would be relatively good. A similar result was obtained in Jutzi et al. (2017).

Jutzi et al. (2017) assumed that the outer disk was dispersed by Neptune immediately after the dispersal of the protosolar nebula, and modeled the collisional evolution over the following 4.5 Gyr. Adopting $q = -2$, they found that the 67P-size body has a 45% chance to avoid a catastrophic disruption, which is in broad agreement with the discussion above. Jutzi et al. (2017) also argued, however, that 67P would have suffered 14–35 *reshaping* impacts (for $q = -2$, the exact number depends on the strength of 67P). If so, the bi-lobed shape of 67P cannot date back to the earliest stages. On the other hand, the number of reshaping impacts is a sensitive function of the unknown number of very small, ~ 100 m projectiles in the Kuiper Belt, and the paucity of small Charon craters seems to indicate that these projectiles are rare (Singer et al. 2018). This may imply that the number of reshaping impacts was much smaller than estimated by Jutzi et al. (2017).

3. Method

Our baseline model is that 67P originally formed as a binary (see discussion in Section 5) and later, by perturbations caused by impacts or dynamical effects, evolved to become a contact binary. Here, we describe the methods that we used to estimate to likelihood of each process, planetary encounters and impacts, to end up as a contact binary.

3.1. Planetary Encounters

N17 developed a model for the origin and dynamical evolution of JFCs. Their simulations started at the time of the protoplanetary gas disk dispersal. The outer planets were assumed to have an initially more compact configuration with Neptune at $\simeq 22$ au. The outer disk of planetesimals was placed at 22–30 au. The outer extension of the disk beyond 30 au was ignored because various constraints indicate that a great majority of planetesimals started at <30 au (see N17 for a discussion). The planetesimal disk was given the mass of 15–20 $M_\oplus$, where $M_\oplus$ is the Earth mass. The disk mass is constrained by the self-consistent simulations of the planetary migration/instability (e.g., Nesvorný & Morbidelli 2012; Deienno et al. 2017) and by Jupiter Trojans (Nesvorný et al. 2013). The size frequency distribution (SFD) of planetesimals was assumed to be a scaled-up version of Jupiter Trojans (Morbidelli et al. 2009a). Each simulation started with 10^6 disk bodies distributed at 22–30 au with the surface density $\Sigma \propto 1/a$.

A two-stage planetary migration/instability model was adopted from Nesvorný & Morbidelli (2012). During the first stage, lasting some 10–30 Myr, planets were migrated on an exponential e-folding timescale τ_1. The dynamical instability was assumed to happen at 10–30 Myr after the start of the simulation. During the instability, Neptune's orbit was modified (see discussion in N17). The integration was then continued with planets migrating to their present orbits on an e-folding timescale τ_2. Eventually, all planets and disk bodies were evolved to $t = 4.5$ Gyr after the gas disk dispersal. The integrations included Galactic tides and stellar encounters.

In the last integration segment, N17 tracked bodies evolving into the inner solar system. To obtain an adequate statistics, bodies reaching orbits with $q < 9$ au and $a < 34$ au were cloned 100 times. N17 used different assumptions on the physical lifetime of active JFCs, including $N_{\rm p}(2.5)$ (see Section 2), the time spent below 2.5 au, or the heliocentric distance weighted effective erosion time, where comets reaching very low perihelion distances were penalized. The results were compared to the known population of active JFCs. N17 found that different parameterizations of the physical lifetime give similar results. Expressed in terms of $N_{\rm p}(2.5)$, the model implies that ~ 1 km JFCs should have 300–800 perihelion passages below 2.5 au before becoming dormant or disrupting, while ~ 10 km JFCs should live longer ($N_{\rm p}(2.5) \sim 3000$).

Here, we repeated two simulations from N17 and monitored *encounters between the disk bodies and planets*. The two simulations had $\tau_1 = 10$ Myr and $\tau_2 = 30$ Myr (Case A) and $\tau_1 = 30$ Myr and $\tau_2 = 100$ Myr (Case B). This covers the interesting range of migration speeds that were inferred from the orbital distribution of the Kuiper Belt (Nesvorný 2015) and giant planet obliquities (Vokrouhlický & Nesvorný 2015, see also Boué et al. 2009). For each encounter within $0.5R_{{\rm H},j}$, where $R_{{\rm H},j}$ is the Hill radius of jth planet ($j = 5$ to 8 from Jupiter to Saturn; the terrestrial planets were not included), the planetocentric orbit of each body was recorded. We selected bodies that became active JFCs in the simulation (according to the criteria of N17). In the second set of simulations, each selected body was assumed to be a binary. The two components of each binary were given masses $M_1 = 1.4 \times 10^{16}$ g and $M_1 = 6.0 \times 10^{15}$ and radii $R_1 = 1.78$ km and $R_2 = 1.33$ km. This corresponds to the physical characteristics of the two lobes of 67P, where the radii and masses were slightly increased to accommodate the estimated past loss of material (Section 2).

To keep things simple, the initial eccentricities of binary orbits were set to zero and the inclinations were selected at random (assuming the isotropic orientation of the binary orbit normal vectors). In different runs, we varied the initial binary semimajor axis, $a_{\rm B}$, between $1 < a_{\rm B}/(R_1 + R_2) < 1000$, or

equivalently $3.11 < a_B < 3110$ km. This covers the whole range of possible initial separations. For reference, the heliocentric Hill radii of an object with the mass $M_1 + M_2 = 2 \times 10^{16}$ g at 5 and 25 au are roughly 1100 and 5600 km, respectively.

Each binary cometesimal was evolved through each encounter recorded in the original simulation. We used the Bulirsch-Stoer *N*-body integrator that was adapted from the Numerical Recipes (Press et al. 1992). The center of mass of the binary cometesimal was first integrated backward from the time of the closest approach to 3 $R_{H,j}$. It was then replaced by the actual binary and integrated forward through the encounter until the planetocentric distance of the binary exceeded 3 $R_{H,j}$. The final binary orbit was used as the initial orbit for the next encounter and the algorithm was repeated over all encounters. The gravity of the Sun and other planets not having an encounter was neglected in these integrations. The tidal evolution of binaries and precession of the binary orbit due to the nonspherical shape of binary components was ignored as well.

We monitored collisions between binary components. If a collision occurred, the integration was stopped and the impact speed and angle were recorded. The binary orbits that became hyperbolic during some stage of the planetary encounter sequence were deemed to be unbound. For the surviving binaries, we recorded the final semimajor axis and eccentricity, which is useful to understand how much perturbation each binary suffered due to planetary encounters. After all integration finished, we combined individual runs into a statistical ensemble of evolutions that expresses the dynamical effects of planetary encounters on binaries. In Section 4, we use these results to discuss the possibility that the bi-lobed shape of 67P is a result of the collapse of 67P's parent binary triggered by planetary encounters.

3.2. Impacts

A small impact into one of the components of a binary can change the binary orbit (Petit & Mousis 2004). The effect of impacts can be especially important for the small and/or loosely bound binaries. For example, the two lobes of 67P, if separated by 20 km from each other, would have the orbital speed of mere $v_B \simeq 0.26\,\mathrm{m\,s^{-1}}$. If a velocity change of this magnitude is delivered to one of the components, the binary would cease to exist. Here, we investigate this process using the collision code that we previously developed (Morbidelli et al. 2009b; Nesvorný et al. 2011).

The code, known as *Boulder* (Morbidelli et al. 2009b), is a statistical particle-in-the-box algorithm that is capable of simulating collisional fragmentation of multiple planetesimal populations. It was developed along the lines of other published codes (e.g., Weidenschilling et al. 1997; Kenyon & Bromley 2001). A full description of the *Boulder* code, tests, and various applications can be found in Morbidelli et al. (2009b), Levison et al. (2009), and Bottke et al. (2010).

In brief, for a given impact between a projectile and a target body, the algorithm computes the specific impact energy Q, defined as the kinetic energy of the projectile divided by the total (projectile plus target) mass. It also computes the critical impact energy, Q_D^*, defined as the energy per unit mass needed to disrupt and disperse 50% of the target. For each collision, the mass of the largest remnant is computed from the scaling laws (e.g., Benz & Asphaug 1999; Leinhardt & Stewart 2009; Stewart & Leinhardt 2009; Jutzi et al. 2017). The mass of the largest fragment and the slope of the power-law SFD of smaller fragments is set as function of Q/Q_D^* by empirical fits to the results of various impact simulations (e.g., Durda et al. 2004, 2007; Nesvorný et al. 2006; also see Bottke et al. 2010).

The Q_D^* function in *Boulder* was assumed to split the difference between the impact simulations of Benz & Asphaug (1999), who used the strong ice, and those of Leinhardt & Stewart (2009), who used the weak ice. To accomplish this, we divided Q_D^* of Benz & Asphaug by a factor, f_Q, where $f_Q = 1$, 3, and 10 were used in different experiments. The main input parameters of the *Boulder* code are the (i) initial SFD of the simulated populations, (ii) intrinsic collision probability, P_i, and (iii) mean impact speed, v_i.

The binary module in the *Boulder* code was described in Nesvorný et al. (2011). The module accounts for small, nondisruptive impacts on binary components and computes the change of the binary orbit depending on the linear momentum of the impactor. The impact velocity vectors are assumed to be randomly oriented in the reference frame of the binary. The changes of orbital elements, δa_B, δe_B and δi_B, are then computed from Equations (7)–(9) in Nesvorný et al. (2011). The binary system is assumed to become unbound if a_B exceeds the Hill radius, or if $e_B > 1$. The code also monitors collisions between components, which occur if $q_B = a_B(1 - e_B) < R_1 + R_2$.

4. Results

4.1. Planetary Encounters

We first discuss the survival of binaries during planetary encounters. Figure 3 shows the survival probability for binaries with $M_1 = 1.4 \times 10^{16}$ g and $M_2 = 6 \times 10^{15}$ g, and different separations. The results in Cases A and B are similar. The survival probability of tight binaries with $a_B < 10$ km is $\simeq$80%. The remaining $\simeq$20% is nearly equally split between two channels of binary removal with either the binary components becoming unbound, or colliding to form a contact binary.

The survival probability drops with increasing separation such that for separations larger than 100 km, the binary survival probability is below 10%. Most loosely bound binaries become unbound. The tightly and loosely bound binaries can be defined by the separation at which the survival probability is 50%. This happens at $a_B \simeq$ 30–50 km or roughly 10–17 times the sum of the component radii, $R_1 + R_2$. The critical distance is slightly smaller in Case A than in Case B, which is related to the richer history of planetary encounters in Case A. The binaries that become unbound do so typically during the early stages of evolution when they have encounters with migrating Neptune.

Interestingly, the probability of collision between components is not a strong function of separation and remains at the $\sim$10% level for the whole range of separations studied here. This is a combination of two opposite trends that offset each other. On one hand, for large separations, the binary orbit needs to reach a very large eccentricity for the two components to collide. On the other hand, it is easier to reach a very large eccentricity for binaries with large separations, because the loosely bound binaries are more susceptible to gravitational perturbations during planetary encounters.

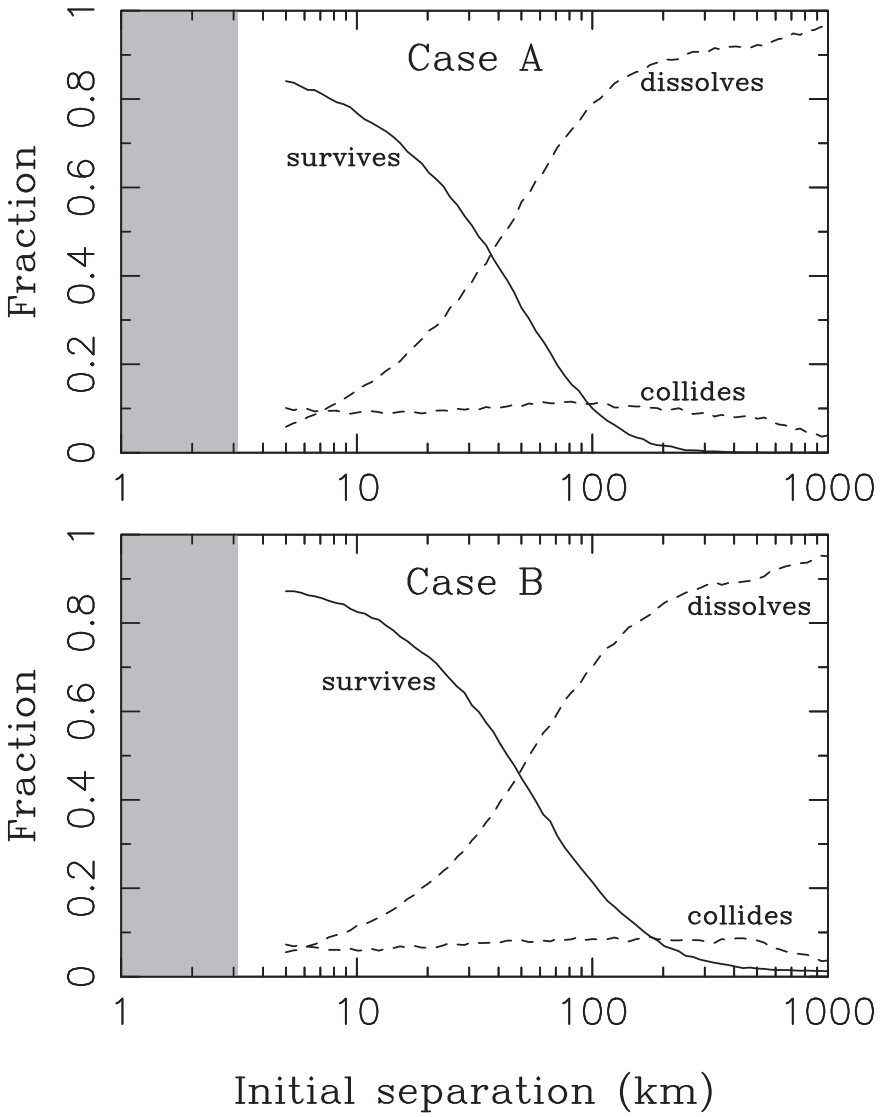

Figure 3. The dynamical survival of 67P-parent binaries during planetary encounters. In the two migration cases A and B, the solid line shows the probability that a binary with given separation survives the whole sequence of planetary encounters. The dashed lines denote the probability that the binary becomes unbound or collapses into a contact binary. The latter outcome happens in ≃10% of cases. The gray box shows where the two components are in contact. We did not investigate binaries with separations below 5 km, where dynamics is strongly influenced by the neglected J_2 term.

Figure 4 shows the mean collision speed between components of the collapsed binaries. The collision speeds are very low, 70–90 cm s^{-1}. For such low speeds, impacts are expected to result in accretion of the binary components. This may happen instantly, during a single head-on collision, or after a series of grazing collisions. If the components have sufficient cohesion before impacts, the end result of this process should be the formation of a contact binary. A detailed investigation of this problem is beyond the scope of this paper.

The significance of these results for 67P depends on the number and properties of small binaries that emerged from the outer planetesimal disk at the time of its dispersal by Neptune. If we assume, for the sake of argument, that most small planetesimals were binaries at this stage of evolution, Figure 3 can be used to make two predictions. First, even under the most optimistic assumptions, the fraction of contact binaries produced by planetary encounters would only be ∼10% (see discussion in Section 5). Second, binaries with the initial separations below ∼100 km would have good chances of survival. If these binaries existed at the beginning of the planetary encounter epoch, we would expect to have several binary comets for each contact binary comet, which is not observed. This implies that the small binaries must have been largely extinct at the time of the planetesimal disk dispersal. Indeed, we show in the following section that impacts during the disk stage are expected to eliminate most small binaries.

4.2. Impacts

Figure 5 shows a test run where the *Boulder* code was used to simulate the collisional evolution of the outer planetesimal disk. Here, we used parameters similar to MR15 to be able to compare the results with MR15 and Section 2. Specifically, we set the intrinsic collision probability $P_i = 8 \times 10^{-21}$ km^{-2} yr^{-1}, mean impact speed $v_i = 0.4$ km s^{-1} and $f_Q = 1$. The initial size distribution of cometesimals was chosen to be similar to the present one, to test how the current distribution would be modified. Specifically, below the break at $D^* = 100$ km, we have $N(>D) = c(D/10\text{km})^{\gamma}$ with $c = 6 \times 10^9$ and $\gamma = -2$. This

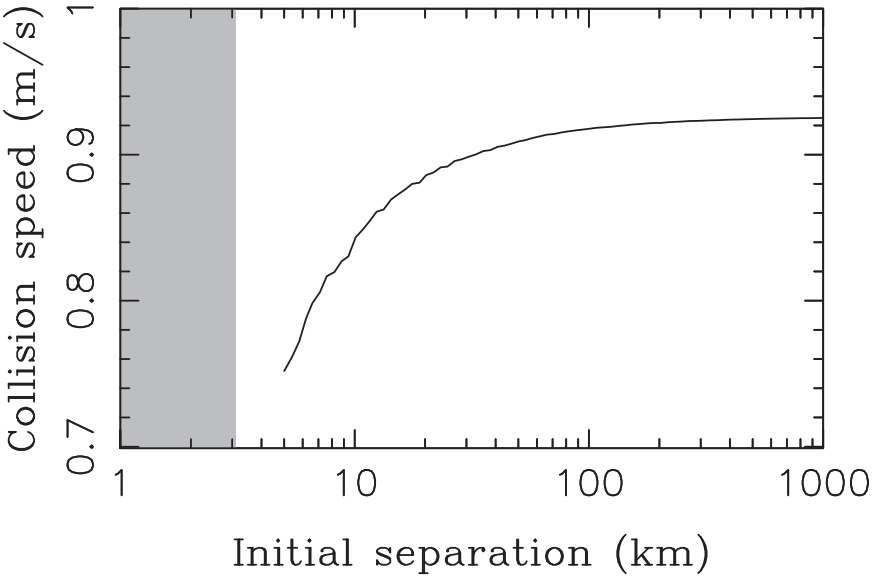

Figure 4. The mean collision speed of the 67P-parent binaries whose components ended colliding with each other.

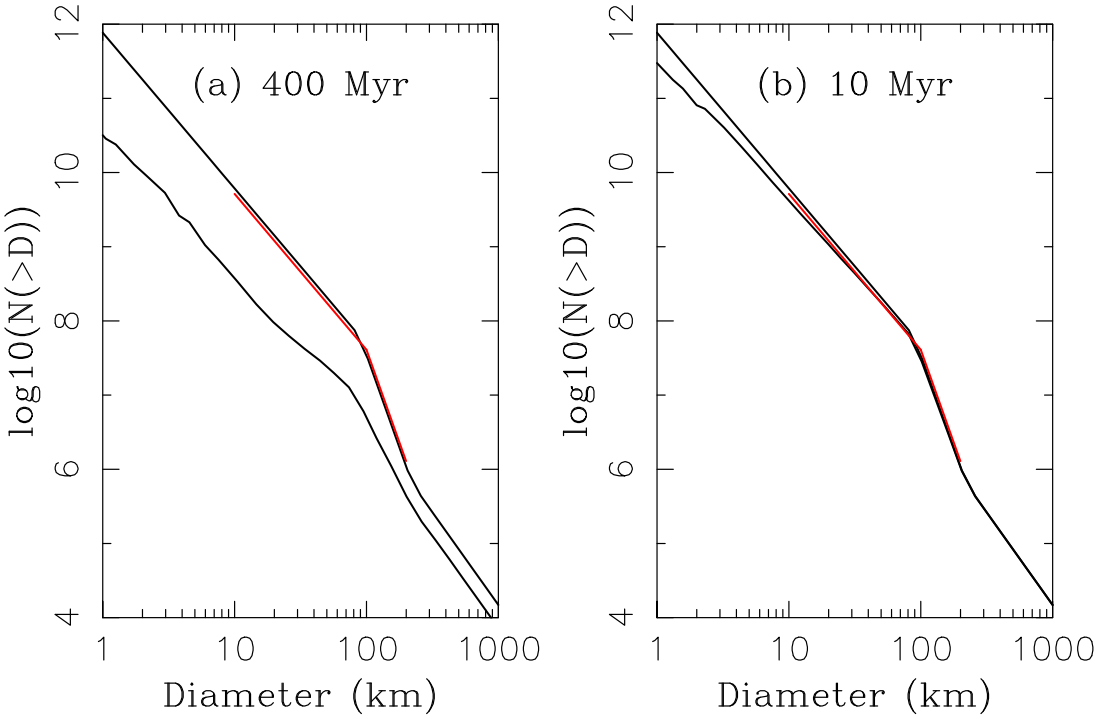

Figure 5. The collisional evolution of the outer planetesimal disk. In panel (a), we assumed that the disk is long-lived (400 Myr). The initial and final size distributions are shown by the upper and lower black lines, respectively. The red line is the target distribution constrained by Jupiter Trojans and planetary migration/instability calculations. Panel (b) shows the same for a short-lived disk (10 Myr).

gives the total initial mass of $20\,M_\oplus$ and roughly 10^{11} cometesimals with $D > 2.3$ km.

If the planetesimal disk is assumed to live for 400 Myr, as in MR15, the number of 67P-size disk bodies is reduced by over a factor of $\simeq$10 over the disk lifetime (Figure 5(a)). In this case, as pointed out by MR15, the survival of 67P is unlikely. In addition, the whole size distribution changes with the final profile being shallower than the initial profile. The final disk mass is $<10\,M_\oplus$, which is a problem, because such a small mass is incompatible with the existing models of the planetary migration/instability (e.g., Nesvorný & Morbidelli 2012), where the disk mass is required to be at least $15\,M_\oplus$. Using a more massive initial disk with a steeper profile could help to alleviate this issue, but we were unable to find an acceptable solution with dozens of initial SFDs that we tested. The main difficulty arises because the more massive disks grind faster and end up with $<10\,M_\oplus$ even if the initial mass is large.

The problems discussed above can be resolved if the planetesimal disk was short-lived. If we adopt, for example, a 10 Myr disk lifetime, the number of 67P-size disk cometesimals drops only by 30% (Figure 5(b)). The survival of 67P is likely in this case, in agreement with the discussion in Section 2. In addition, the disk mass is only modestly reduced from $20\,M_\oplus$ to $\simeq 19\,M_\oplus$. Thus, a short-lived planetesimal disk

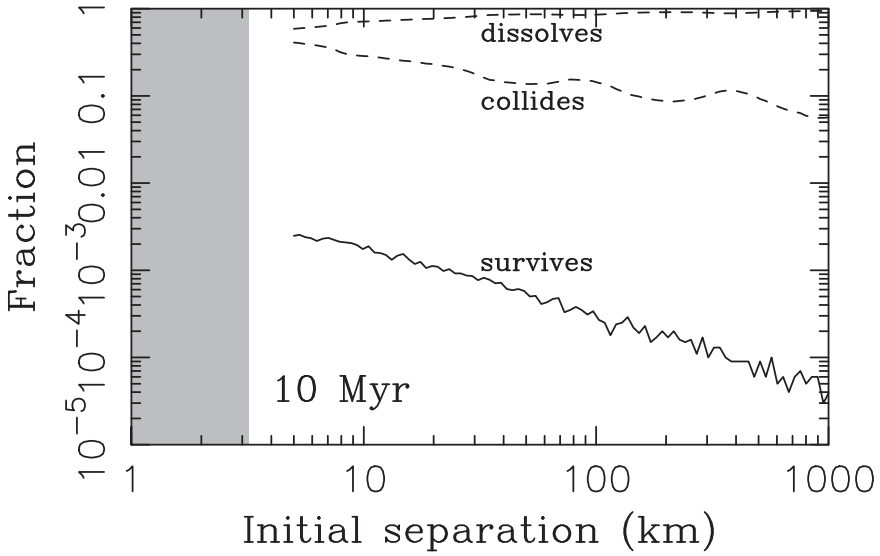

Figure 6. The survival of 67P-parent binaries during the collisional evolution of the outer planetesimal disk. Here, we assumed that the outer disk lasts 10 Myr before it is dispersed by Neptune. The solid line shows the surviving binary fraction. The dashed lines denote the fraction of binaries collapsing into contact binaries and those becoming unbound.

may provide a more consistent framework for the early evolution of the solar system than the one adopted in MR15. Similar results were already reported in Jutzi et al. (2017). They found that the probability of 67P to avoid a disruptive collision is 30%–70% (for a short-lived disk and $q = -2$).

Figure 6 illustrates the survival of 67P-parent binaries during the collisional evolution of the outer disk. Following MR15, we adopted $P_i = 8 \times 10^{-21}\,\mathrm{km^{-2}\,yr^{-1}}$, $v_i = 0.4\,\mathrm{km\,s^{-1}}$ and $f_Q = 1$. The disk lifetime was assumed to be 10 Myr. In this case, the surviving binary fraction is $\simeq 2 \times 10^{-3}$ for the tight binaries ($a_\mathrm{B} < 10$ km) and $\sim 10^{-4}$ for the loose binaries ($a_\mathrm{B} = 100$–1000 km). The most likely outcome of impacts is that the binary orbit becomes unbound. For about 30% of the tight binaries, the binary components end up colliding with each other. This fraction decreases to ~10% for the wide binaries. The collisional speeds between components of the collapsed binaries are gentle and show a trend similar to that in Figure 4.

When the disk lifetime is increased to 20 Myr, the fraction of surviving binaries drops below 10^{-5}, which is the resolution limit of this study (the *Boulder* code was set to have 10^5 binaries for each initial separation). The fraction of collapsed binaries remains ~10% for the wide binaries and ≃30% for the tight binaries. The remaining 70%–90% of binaries become unbound. The results do not change much when even longer disk lifetimes are considered; however, in the cases with >30 Myr lifetimes, most 67P-size cometesimals become catastrophically disrupted (NR15), and the disk's SFD starts to diverge from the one imposed by the observational constraints (Figure 5).

We performed several additional runs with the *Boulder* code to test how the results depend on various parameters. For example, when v_i is decreased from the nominal $0.4\,\mathrm{km\,s^{-1}}$ to $0.2\,\mathrm{km\,s^{-1}}$, to simulate the dynamically cold disk conditions, we find that the fraction of tight binaries that survive after 10 Myr of the collisional evolution is ≃0.01, about a factor of 5 higher than in the case with $v_i = 0.4\,\mathrm{km\,s^{-1}}$. This shows that the fraction of surviving binaries is a sensitive function of v_i. The fractions of unbound and collapsed binaries with $v_i = 0.2\,\mathrm{km\,s^{-1}}$ are similar to and follow the same trends as those obtained with $v_i = 0.4\,\mathrm{km\,s^{-1}}$ (e.g., 30% of tight binaries collapse into contact binaries).

4.3. Kozai Cycles

The Kozai dynamics of a binary orbit arises due to the gravitational potential of the Sun (see Naoz 2016 for a review). In the simplest quadrupole approximation of the solar gravity field, the quantity $(1 - e_\mathrm{B}^2)^{1/2} \cos i_\mathrm{B}$ is conserved and the problem is integrable. For a trajectory starting with $e_\mathrm{B} = 0$ and $i_{\mathrm{B},0}$, the maximum eccentricity that can be reached during the Kozai cycles is $e_{\mathrm{B,max}} = (1\text{–}5/3 \cos^2 i_{\mathrm{B},0})^{1/2}$. For the the two components to collide, $q_\mathrm{B} < R_1 + R_2$. This defines a critical value, i_B^*, where $\cos^2 i_\mathrm{B}^* = 3/5(1 - (1 - (R_1 + R_2)/a_\mathrm{B})^2)$. If the initial inclination, $i_{\mathrm{B},0}$, is larger than i_B^*, the two components will collide. If $i_{\mathrm{B},0} < i_\mathrm{B}^*$, on the other hand, q_B will not drop below $R_1 + R_2$ and the binary system will survive. Assuming an isotropic initial distribution of $i_{\mathrm{B},0}$, the survival probability as a function of separation is shown in Figure 7.

In addition, for the Kozai cycles to be effective, the two binary components must be roughly spherical and/or the binary separation must be large. If not, the gravitational potential from J_2 of the binary components will prevail over the solar gravity, resulting in a simple precession of the binary orbit pole about the heliocentric orbit pole. The critical semimajor axis is $a_\mathrm{B}^* = (2\mu J_2 R^2 a_\mathrm{h}^3)^{1/5}$, where μ is the binary-to-Sun mass ratio, and a_h is the semimajor axis of the heliocentric orbit (e.g., Mignard 1982). The J_2R^2 term is the measure of nonsphericity of the binary components. For a homogeneous ellipsoid with axes $a > b > c$, $J_2R^2 = (a^2 + b^2 - 2c^2)/10$. Summing up the contributions from the measured shapes of the two lobes of 67P we have $J_2R^2 \simeq 0.67\,\mathrm{km^2}$. In Figure 7, we plot $a_\mathrm{B}^* = 260$ km corresponding to $J_2R^2 = 0.67\,\mathrm{km^2}$, $\mu = 10^{-17}$ and $a_\mathrm{H} = 25$ au.

It is apparent from Figure 7 that the survival of a 67P-parent binary is likely for all initial separations. For small separations, the fast apsidal precession due to J_2 renders the Kozai cycles ineffective. At large separations, the collision orbits do not represent an important volume in space of initial conditions, because the orbital eccentricity must become very large for the

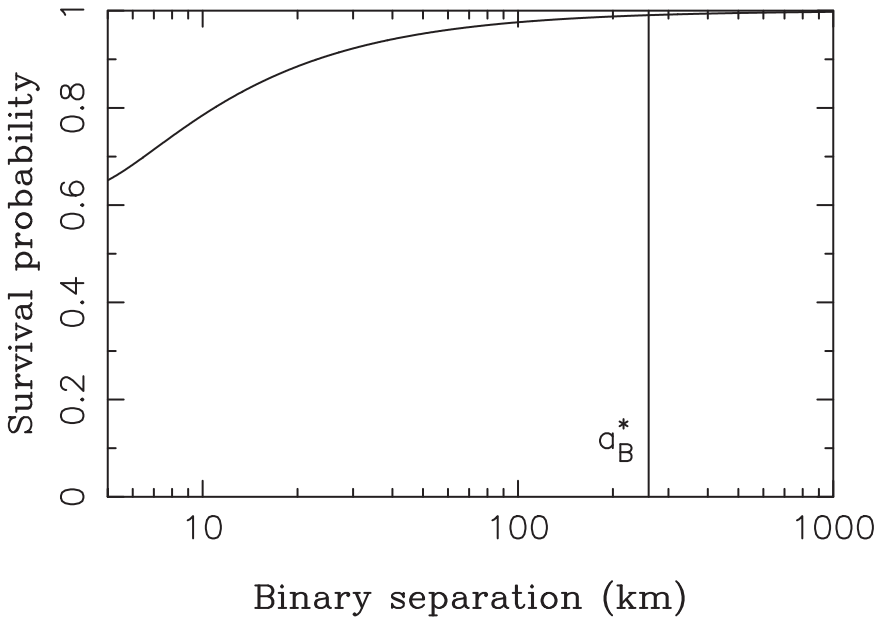

Figure 7. The survival of 67P-parent binaries against Kozai-induced collisions between components. The initial orientations of the binary orbits were assumed to be random. The vertical solid line shows the transition between the J_2-dominated dynamics for small separations to the Kozai-dominated dynamics for large separations. See Section 4.3 for the parameter values adopted in this plot.

collision to occur. This happens only if the initial inclination of the binary orbit is very close to 90° (relative to the heliocentric orbit). We therefore conclude that the Kozai dynamics should play a only minor role.

5. Discussion and Conclusions

We postulated that 67P formed as a binary and evaluated the probability that the binary orbit was destabilized by collisional and dynamical processes. Whether 67P actually formed as a binary is unclear. On one hand, binaries are common among the 100 km-class CCs at 40–50 au. The formation of CC binaries is thought to be related to the accretion processes in the early solar system (e.g., Goldreich et al. 2002; Nesvorný et al. 2010). The present-day fraction of binaries in the CC population is estimated to be 30%–100% (e.g., Noll et al. 2008; Fraser et al. 2017). The CC binaries survived to the present day because the 40–50 au region presumably received only modest perturbations from the collisional and dynamical processes.

On the other hand, 67P formed significantly closer to the Sun, probably in the 20–30 au disk, and is much smaller than the observed CC binaries. To establish whether 67P formed as a primordial binary, we would therefore need to understand how the accretion processes scale with the heliocentric distance and size. For example, planetesimals may have formed by the streaming instability followed by gravitational collapse (Youdin & Goodman 2005; Youdin & Johansen 2007). If so, it would probably be reasonable to assume that their formation at 20–30 au and 40–50 au followed the same suit, because the streaming instability is not expected to have a strong dependence on the heliocentric distance.

Also, Simon et al. (2017) and others showed that the streaming instability is capable of forming planetesimals of different sizes with the expected SFD scaling that is similar to the observed SFD of the Kuiper Belt objects and Jupiter Trojans below 100 km. This may suggest that the formation of 67P-size cometesimals was just a scaled-down version of the formation of 100 km CCs. (Note that the existing streaming instability simulations do not have the required resolution to explicitly demonstrate the formation of km size cometesimals.) These arguments may provide some justification to our assumption that 67P formed as a binary. In contrast, the high-resolution simulations of the streaming instability show that small clumps of pebbles can be easily dispersed by turbulent diffusion (Klahr & Schreiber 2016). If so, the formation of the 67P-size cometesimals by the streaming instability may be inefficient. Other accretion models, including the hierarchical coagulation by two-body collisions, may have different implications (see Youdin & Kenyon 2013).

The expected fraction of contact binaries among JFCs is the product of: (1) the fraction of cometesimals that formed as binaries, $f_{\rm binary}$, and (2) the fraction of binaries that collapsed to become contact binaries, $f_{\rm contact}$. The main contribution of this work was to estimate $f_{\rm contact}$ for the 67P-class comets. We found that small impacts during the collisional evolution of the outer disk at 20–30 au give $f_{\rm contact} = 10\%$–30% (for the range of the initial binary separations and outer disk lifetimes considered here). The disk lifetimes $\lesssim 10$ Myr are required for 67P to avoid a catastrophic disruption (MR15 and Section 2). Thus, for example, if $f_{\rm binary} \sim 0.5$, the expected fraction of 67P-like contact binaries among JFCs would be $\sim$5%–15%.

While the processes described here could potentially explain the bi-lobed shape of 67P, they are probably not efficient enough to explain the shapes of comets in general. Six comets were imaged by spacecraft and have good shape models: 1P/Halley, 9P/Tempel 1, 19P/Borrely, 67P, 81P/Wild 2, and 103P/Hartley 2. Of these, 67P stands as the one with the most bi-lobed shape. Halley, Borrelly, and Hartley 2 are also bi-lobed but less clearly so than 67P. Wild 2 and Tempel 1 are more rounded. These observations therefore indicate that four out of six, or roughly 67% of comets appear to be bi-lobed, which is a much larger fraction than the one expected from the statistics of collapsed binaries (see above). This suggests that

other, more efficient mechanism must be at play (e.g., Jutzi & Benz 2017; Schwartz et al. 2018).

Only a very small fraction ($<2 \times 10^{-3}$ for $v_i = 0.4\,\mathrm{km\,s^{-1}}$ and $\gtrsim$10 Myr lifetime) of 67P-parent binaries survive the collisional evolution of the outer planetesimal disk. The surviving binaries undergo gravitational perturbations during planetary encounters and are further reduced in number. The survival during planetary encounters depends on the initial binary separation: most tight binaries with $a_B < 30$–$50\,\mathrm{km}$ survive, while most $a_B > 30$–$50\,\mathrm{km}$ are dissolved (Figure 3). The probability to become a contact binary is ∼10% during this stage. Given that the number of binaries was severely reduced during the previous stage of the collisional evolution, the relevance of planetary encounters for the contact binary formation must be relatively minor.

In addition, we find that it is very unlikely that 67P is a new comet that evolved on a JFC orbit in the past century. We estimate that the probability that it evolved onto an orbit with $q < 2.5$ au in the past 1000 years is only 10%.

This work was supported by funding for the Rosetta-Alice project from NASA via Jet Propulsion Laboratory contract 1336850 to the Southwest Research Institute. We thank A. Morbidelli for a helpful referee report.

References

Benz, W., & Asphaug, E. 1999, Icar, 142, 5
Blum, J., Gundlach, B., Krause, M., et al. 2017, MNRAS, 469, S755
Bottke, W. F., Nesvorný, D., Vokrouhlický, D., & Morbidelli, A. 2010, AJ, 139, 994
Boué, G., Laskar, J., & Kuchynka, P. 2009, ApJL, 702, L19
Brasser, R., & Morbidelli, A. 2013, Icar, 225, 40
Davidsson, B. J. R., Sierks, H., Güttler, C., et al. 2016, A&A, 592, A63
Deienno, R., Morbidelli, A., Gomes, R. S., & Nesvorný, D. 2017, AJ, 153, 153
Durda, D. D., Bottke, W. F., Enke, B. L., et al. 2004, Icar, 167, 382
Durda, D. D., Bottke, W. F., Nesvorný, D., et al. 2007, Icar, 186, 498
Fraser, W. C., Bannister, M. T., Pike, R. E., et al. 2017, NatAs, 1, 0088
Goldreich, P., Lithwick, Y., & Sari, R. 2002, Natur, 420, 643
Guzzo, M., & Lega, E. 2017, MNRAS, 469, S321
Johansen, A., Youdin, A., & Mac Low, M.-M. 2009, ApJL, 704, L75
Johansen, A., Youdin, A. N., & Lithwick, Y. 2012, A&A, 537, A125
Jorda, L., Gaskell, R., Capanna, C., et al. 2016, Icar, 277, 257
Jutzi, M., & Benz, W. 2017, A&A, 597, A62
Jutzi, M., Benz, W., Toliou, A., Morbidelli, A., & Brasser, R. 2017, A&A, 597, A61
Kaib, N. A., & Sheppard, S. S. 2016, AJ, 152, 133
Kenyon, S. J., & Bromley, B. C. 2001, AJ, 121, 538
Klahr, H., & Schreiber, A. 2016, IAU Symp. 318, Asteroids: New Observations, New Models (Cambridge: Cambridge Univ. Press), 1
Leinhardt, Z. M., & Stewart, S. T. 2009, Icar, 199, 542
Levison, H. F., Bottke, W. F., Gounelle, M., et al. 2009, Natur, 460, 364
Levison, H. F., & Duncan, M. J. 1997, Icar, 127, 13
Levison, H. F., Morbidelli, A., Tsiganis, K., Nesvorný, D., & Gomes, R. 2011, AJ, 142, 152
Maquet, L. 2015, A&A, 579, A78
Massironi, M., Simioni, E., Marzari, F., et al. 2015, Natur, 526, 402
Mignard, F. 1982, Icar, 49, 347
Morbidelli, A., Bottke, W. F., Nesvorný, D., & Levison, H. F. 2009a, Icar, 204, 558
Morbidelli, A., Levison, H. F., Bottke, W. F., Dones, L., & Nesvorný, D. 2009b, Icar, 202, 310
Morbidelli, A., Nesvorný, D., et al. 2018, Icar, in press
Morbidelli, A., & Rickman, H. 2015, A&A, 583, A43, (MR15)
Naoz, S. 2016, ARA&A, 54, 441
Nesvorný, D. 2015, AJ, 150, 73
Nesvorný, D., Enke, B. L., Bottke, W. F., et al. 2006, Icar, 183, 296
Nesvorný, D., & Morbidelli, A. 2012, AJ, 144, 117
Nesvorný, D., Roig, F., & Bottke, W. F. 2017b, AJ, 153, 103
Nesvorný, D., & Vokrouhlický, D. 2016, ApJ, 825, 94
Nesvorný, D., Vokrouhlický, D., Bottke, W. F., Noll, K., & Levison, H. F. 2011, AJ, 141, 159
Nesvorný, D., Vokrouhlický, D., Dones, L., et al. 2017, ApJ, 845, 27, (N17)
Nesvorný, D., Vokrouhlický, D., & Morbidelli, A. 2013, ApJ, 768, 45
Nesvorný, D., Youdin, A. N., & Richardson, D. C. 2010, AJ, 140, 785
Noll, K. S., Grundy, W. M., Chiang, E. I., Margot, J.-L., & Kern, S. D. 2008, in The Solar System Beyond Neptune, ed. M. A. Barucci et al. (Tucson, AZ: Univ. Arizona Press), 345
Paetzold, M., Andert, T., Hahn, M., et al. 2016, AAS/DPS Meeting 48 Abstracts, 116.27
Parker, A. H., & Kavelaars, J. J. 2010, ApJL, 722, L204
Petit, J.-M., & Mousis, O. 2004, Icar, 168, 409
Press, W. H., Teukolsky, S. A., Vetterling, W. T., & Flannery, B. P. 1992, Numerical recipes in FORTRAN. The art of scientific computing (2nd ed.; Cambridge: Cambridge Univ. Press)
Rickman, H., Marchi, S., A'Hearn, M. F., et al. 2015, A&A, 583, A44
Schwartz, S. R., Michel, P., Jutzi, M., et al. 2018, NatAs, 2, 379
Simon, J. B., Armitage, P. J., Youdin, A. N., & Li, R. 2017, ApJL, 847, L12
Singer, K. N., McKinnon, W. B., Gladman, B., et al. 2018, Sci, in press
Stewart, S. T., & Leinhardt, Z. M. 2009, ApJL, 691, L133
Vokrouhlický, D., & Nesvorný, D. 2015, ApJ, 806, 143
Weidenschilling, S. J., Spaute, D., Davis, D. R., Marzari, F., & Ohtsuki, K. 1997, Icar, 128, 429
Youdin, A., & Johansen, A. 2007, ApJ, 662, 613
Youdin, A. N., & Goodman, J. 2005, ApJ, 620, 459
Youdin, A. N., & Kenyon, S. J. 2013, in Planets, Stars and Stellar Systems, Vol. 3, Solar and Stellar Planetary Systems, ed. T. D. Oswalt, L. M. French, & P. Kalas (Dordrecht: Springer), 1